Journal of Structural Geology 33 (2011) 985–999

Contents lists available at ScienceDirect

Journal of Structural Geology

journal homepage: www.elsevier.com/locate/jsg

Structurally controlled fluid flow: High-grade silver ore-shoots at Martha epithermal mine, Deseado Massif, Argentina

G.N. Páez [a,b,*], R. Ruiz [a,b], D.M. Guido [a,b], S.M. Jovic [a,b], I.B. Schalamuk [a,b]

[a] Instituto de Recursos Minerales (INREMI), Universidad Nacional de La Plata, Calle 64 esquina Calle 120, (1900) La Plata, Provincia de Buenos Aires, Argentina
[b] Consejo Nacional de Investigaciones Científicas y Técnicas (CONICET), Buenos Aires, Argentina

ARTICLE INFO

Article history:
Received 31 August 2010
Received in revised form
1 February 2011
Accepted 18 February 2011
Available online 2 March 2011

Keywords:
Epithermal veins
Normal faults
Hydrothermal flow
Ore-shoots
Jurassic
Patagonia

ABSTRACT

The role of structurally controlled fluid flow during epithermal ore-shoot formation is addressed through a structural study of the high grade Martha Mine epithermal deposit (Deseado Massif, Patagonia, Argentina). Martha is a silver-rich deposit, characterised by a complex mineralogy dominated by Ag–As–Sb sulphosalts and Cu–Pb–Zn sulphides. Mineralised veins can be subdivided into two groups: master structures that trend approximately NW–SE, and second-order structures that trend E–W and coalesce into the master structures. The Martha vein system is interpreted as a hard-linked step-over zone between two NW–SE trending fault segments. Furthermore, the geometry of ore-shoots at Martha Mine suggests a first-order structural control on their location and orientation. At the deposit scale, mineralisation is concentrated in the step-over zone. Mineralisation, and presumably hydrothermal fluid flow, was concentrated at the intersection between the two main vein groups. Finally, at the scale of single veins, jogs and subordinate step-overs were important channels for hydrothermal fluids and the formation of high-grade ore-shoots.

1. Introduction

Epithermal veins are the result of mineral deposition from circulating hydrothermal solutions that percolate through interconnected fault systems and fracture meshes (e.g. Sillitoe and Hedenquist, 2003; Cox, 2005; Simmons et al., 2005; Micklethwaite et al., 2010); therefore, the study of these deposits offers a unique possibility to analyse structural controls on hydrothermal circulation, providing insights on where and how fluid pathways are generated on shallow crustal levels.

Epithermal deposits generally originate in close affiliation with volcanism and normal faulting, within shallow magmatic/hydrothermal systems, in a broad spectrum of tectonic settings (Sillitoe and Hedenquist, 2003; Simmons et al., 2005). Epithermal deposits host both precious and base metals, but they are currently being mined mostly for their gold and silver contents, with almost 6% of the world's Au and 16% of its Ag production coming from this type of ore deposit (Simmons et al., 2005).

In these shallow hydrothermal environments, ore bodies tend to be irregular in shape and strongly influenced by zones of high permeability, which can be controlled either by structure and/or lithology (Reid et al., 1975; Brathwaite et al., 2001; Oliver et al., 2001; Simmons et al., 2005). In extensional environments it is likely that epithermal veins develop in close association with normal faults (e.g. Sillitoe and Hedenquist, 2003; Christie et al., 2007). These structures may act as zones of enhanced permeability, serving both as conduits for hydrothermal fluids and deposition sites for hydrothermal minerals (Cox, 2005; Micklethwaite et al., 2010).

Normal faults commonly develop through the evolution of segmented arrays (Pollard et al., 1982; Gibbs, 1984; Rosendahl et al., 1986; Childs et al., 1996; Walsh et al., 1999; Peacock, 2002; Walsh et al., 2003; Nicol et al., 2010; Faulkner et al., 2010); therefore, fault geometry is strongly influenced by segment linkage during fault propagation. In this scenario, segments can link both along dip and/or along strike, giving rise to a 3D curviplanar fault geometry characterised by the development of bends, relay ramps and splays between several overlapping or underlapping fault segments (Childs et al., 1996; Walsh et al., 1999; Ferrill and Morris, 2003; Micklethwaite, 2009; Nicol et al., 2010; Faulkner et al., 2010).

Within structurally controlled epithermal deposits, hydrothermal flow direction through the host rocks is governed by

* Corresponding author. Instituto de Recursos Minerales (INREMI), Universidad Nacional de La Plata, Calle 64 esquina Calle 120, (1900) La Plata, Provincia de Buenos Aires, Argentina. Tel./fax: +54 221 4225648.
E-mail addresses: marduk_paez@yahoo.com.ar, gerardo_paez@hotmail.com (G.N. Páez).

0191-8141/$ – see front matter © 2011 Elsevier Ltd. All rights reserved.
doi:10.1016/j.jsg.2011.02.007

hydraulic gradient and interconnections between discontinuities (Sibson, 1996; Cox, 2005). However, the presence of irregularities, jogs and intersections within structures may localise pathways for hydrothermal solutions to be focused and concentrated (Hulin, 1929; Sibson, 1996; Rowland and Sibson, 2004; Cox, 2005; Faulkner et al., 2010). The presence of highly permeable conduits combined with an efficient ore deposition mechanism is considered to be critical in order to form an economic-grade deposit (Simmons and Browne, 2000; Berger et al., 2003; Cox, 2005; Simmons and Brown, 2006; Micklethwaite, 2009).

Therefore, the understanding of nucleation and propagation of normal faults and how this process controls ore deposition is a key point to understand epithermal vein and ore-shoots formation. Even so, few detailed studies have been published dealing with structural aspects controlling fluid pathways and ore-shoot formation in shallow epithermal environments (e.g. Berger et al., 2003; Chauvet et al., 2006; Begbie et al., 2007; Kolb and Hagemann, 2009).

This research addresses the role of structurally controlled fluid flow and ore-shoot formation during epithermal mineralisation in an extensional environment. In this paper, we present a structural description based on field mapping, vein infill studies, vein opening analysis, and ore-shoot distribution to delineate a model for the evolution of Martha Mine silver mineralisation. Also, we analyse structural controls on grade distributions in one of the richest silver deposits of Argentinean Patagonia, with significant implications for future exploration activities in the Deseado Massif and other epithermal districts.

2. The Deseado Massif

2.1. Regional geology

The Deseado Massif (Fig. 1) is a 60,000 km^2 geological region located in the southern part of Extra-Andean Patagonia in the central portion of Santa Cruz province. During the Middle to Upper Jurassic (177.8–150.6 Ma; Pankhurst et al., 2000), a volcanic mega-event occurred in Patagonia giving rise to the Chon Aike Large Igneous Province (Pankhurst et al., 1998, 2000). In the Deseado Massif, this event is represented by a volcanic suite that was named the Bahía Laura Volcanic Complex (BLVC; Fig. 1) by Feruglio (1949) and Guido (2004). Pyroclastic rocks predominate within the BLVC, with subordinate amounts of intercalated lavas of andesitic to rhyolithic composition, and with a calcalkaline, peraluminous and high potassium signature (Pankhurst et al., 1998; Guido, 2004). Intricate stratigraphic relationships characterise this complex, with multiple intercalations of different rock facies (Echeveste et al., 2001; López, 2006; Ruiz et al., 2008; Wallier, 2009).

2.2. Structure

The Meso-Cenozoic tectonic evolution of the Deseado Massif is dominated by two main tectonic regimes (Giacosa et al., 2010). First a Jurassic tectonic phase occurred (Middle to Upper Jurassic), which structurally imprinted large areas of Southern Gondwana with a general SW–NE extensional axis. Crustal extension produced dextral-extension along WNW oriented first-order faults and sinistral- to pure-extension on second-order NW oriented faults (López, 2006; Moreira et al., 2008; Giacosa et al., 2010). The Jurassic extensional environments and volcanism were a consequence of both continued back-arc extension related to Pacific margin subduction, and regional extension related to opening of the Atlantic Ocean during the initial stages of the Gondwanan supercontinent break-up (Pankhurst et al., 2000; Homovc and Constantini, 2001; Richardson and Underhill, 2002). Two post-Jurassic Andean-related tectonic phases occurred along a SW–NE to W–E compressional axis, and are dominated by sinistral transpression on pre-existing WNW normal faults, and reverse reactivation of some NW and N–S trending normal faults (Homovc and Constantini, 2001; Giacosa et al., 2010).

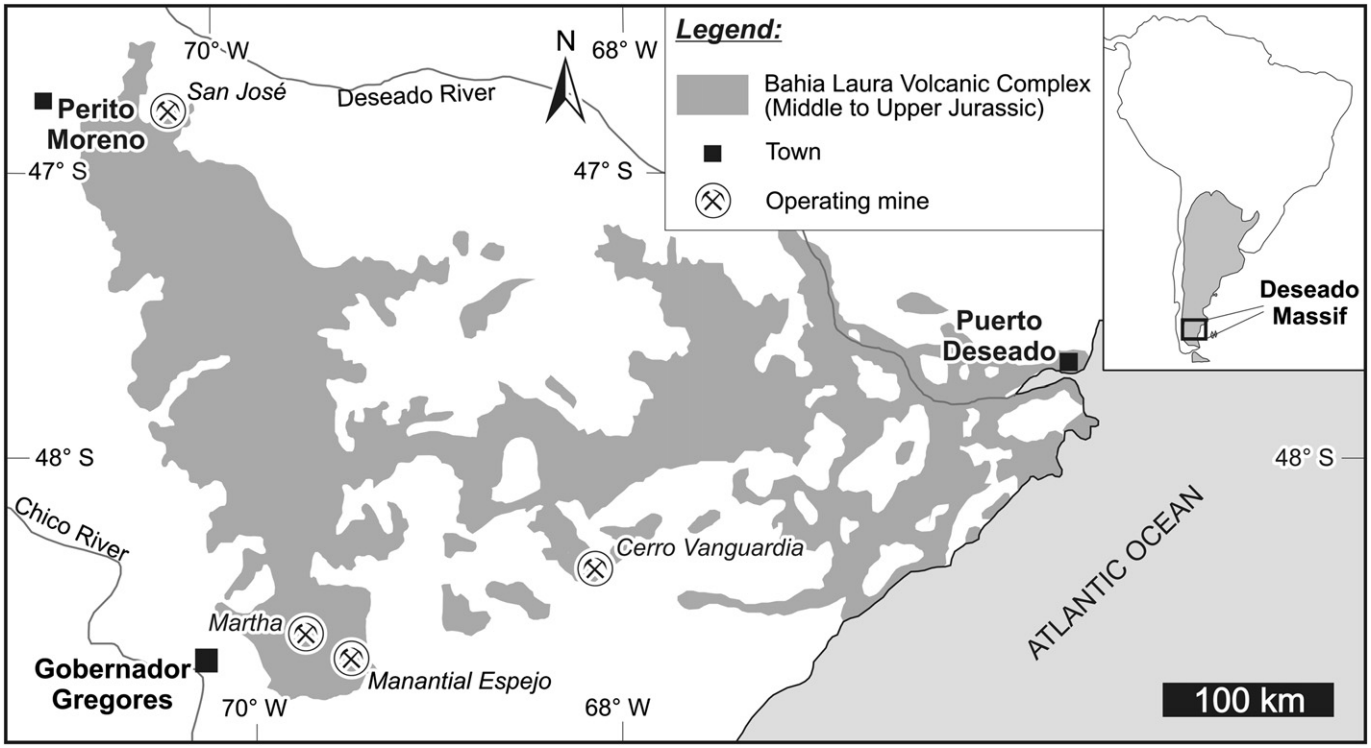

Fig. 1. Simplified geological map of the Deseado Massif showing distribution of Jurassic volcanic rocks and location of the four producing mine sites.

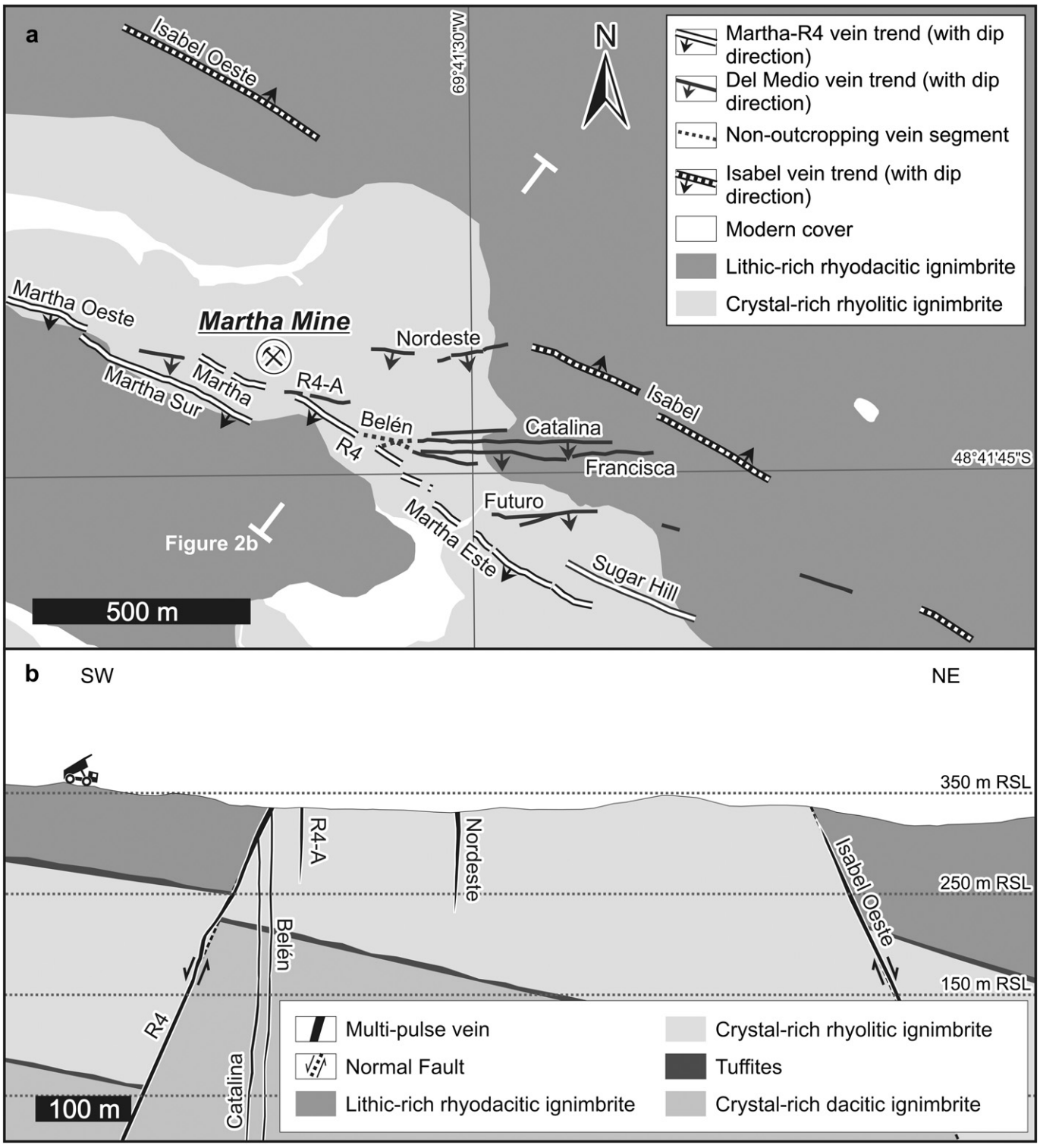

Fig. 2. (a) Geological map of Martha Mine silver-rich epithermal deposit. (b) SW–NE trending cross-section showing lithology and vein distribution. Altitude is in metres with respect to sea level (m RSL).

2.3. The Deseado metallogenic province

The BLVC contains numerous gold and silver epithermal deposits, leading Schalamuk et al. (1999) to define the Deseado Massif as an Au–Ag metallogenic province. The majority of the Au–Ag occurrences are low sulphidation (LS) style (Guido and Schalamuk, 2003; Echavarría et al., 2005; Fernández et al., 2008), but in the past few years intermediate sulphidation and polymetallic deposits also have been reported (Gonzalez Guillot et al., 2004; Guido et al., 2005; Jovic et al., 2010). Mineralisation typically occurs as veins, veinlets, vein stockworks and breccias which are strongly controlled by Jurassic rift structures, showing dominant NW and WNW orientations with

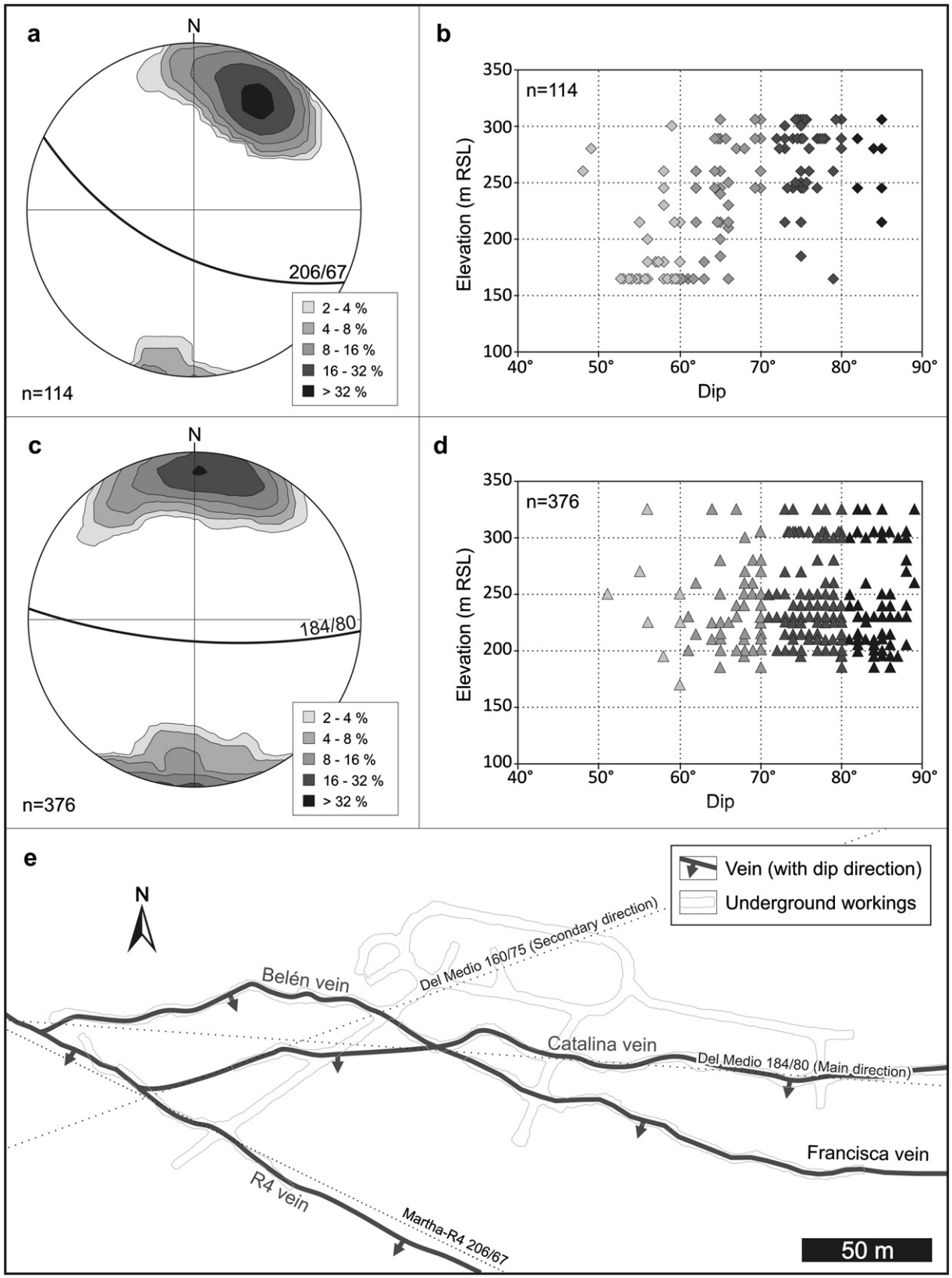

Fig. 3. (a) Contoured lower hemisphere equal-area stereonet, showing orientation of structures within the Martha-R4 vein trend. (b) Vein dip data of Martha-R4 vein trend relative to altitude in metres with respect to sea level (m RSL); gray scale shading used for different dips. (c) Contoured lower hemisphere equal-area stereonet, showing orientation of structures within the Del Medio vein trend. (d) Vein dip data of Del Medio vein trend relative to altitude in metres with respect to sea level (m RSL); gray scale shading used for different dips. (e) Geological sketch map of the 185 m underground level of Martha Mine showing the three main directions found in Martha Mine veins.

Table 1
Paragenetic scheme of Martha Mine epithermal mineralization.

	Vein episode			
	E_1	E_2	E_3	E_4
Vein volume[a]	Less than 5%	Up to 20%	Up to 95%	Up to 30% (only documented in Martha-R4 vein trend)
Ore mineralogy	–	Pyrite, sphalerite, chalcopyrite, galena, silver bearing tetraedrite (freibergite), polibasite, pyrargirite, miargyrite, native silver, electrum	–	Pyrargirite, miargirite, native silver, minor sphalerite and chalcopyrite
Sulfide content	None	High, with a progressive decreasing sulfide content	None	Variable, high only when developed in proximity to E2
Gangue minerals	Quartz with minor adularia	Adularia with minor quartz and sericite	Adularia with minor quartz and sericite	Chalcedony
Vein textures	Massive	Breccia, minor crustiform banding	Massive, breccia, minor crustiform banding, localized drusy cavities	Breccia
Breccia matrix/clast ratio	–	Moderated	High	Low
Alteration assemblage	None	Adularia + silicification	Illite + silicification + smectite	Silicification

[a] Volume percentage within multipulse veins.

minor influence by NE and E–W directed structures. Associated with the epithermal veins, widespread hot spring deposits are present (Schalamuk et al., 1997).

Over the past 12 years, the Deseado Massif has produced more than 3 million oz of gold and over 40 million oz of silver from four operational mines (Cerro Vanguardia, Martha, Manantial Espejo and San José; Fig. 1). Most of the precious metals have been extracted from Cerro Vanguardia Mine (about 77%, producing since 1998), followed by 11% from Martha Mine (producing since 2001), and the remaining 12% from San José and Manantial Espejo mines (producing since 2008 and 2009, respectively). This is a relatively young gold and silver producing region, and it has great potential for expanding its known resources, as there are currently more than 50 prospects undergoing different stages of exploration.

3. Methodology

Martha Mine veins were studied by evaluating mine level plan maps, cross-sections, longitudinal sections, and 3D models of the ore bodies and surrounding geology (data provided by Coeur d'Alene Mines Corporation). This preliminary study was followed by surface mapping at 1:2500 scale over the entire property, with detailed mapping undertaken at accessible underground levels and stopes at 1:500 and 1:100 scales. Crosscutting relationships between the different hydrothermal stages were examined by logging available drill cores at the mine site and also from mapping of underground exposures.

Longitudinal sections analysed in this work were calculated from a three-dimensional solid geological model by Sims (2010) using the inverse distance to the 3rd power interpolation method, with the utilisation of isotropic search ellipsoids and a high-grade transition model to restrict the range of influence of high-grade values (Sims, 2010). Finally, the geometry of the ore-shoots was controlled using geological information from underground levels and stopes, and grade-control assays from extractive activities.

All observations and interpretations were complemented by data from grade-control records and exploration drill holes, and compiled into a GIS database. Finally, all structural data were plotted and analysed using the software Georient v9.4.4 (Holcombe, 2009). All orientations herein are given as dip-direction/dip (e.g. 206/67).

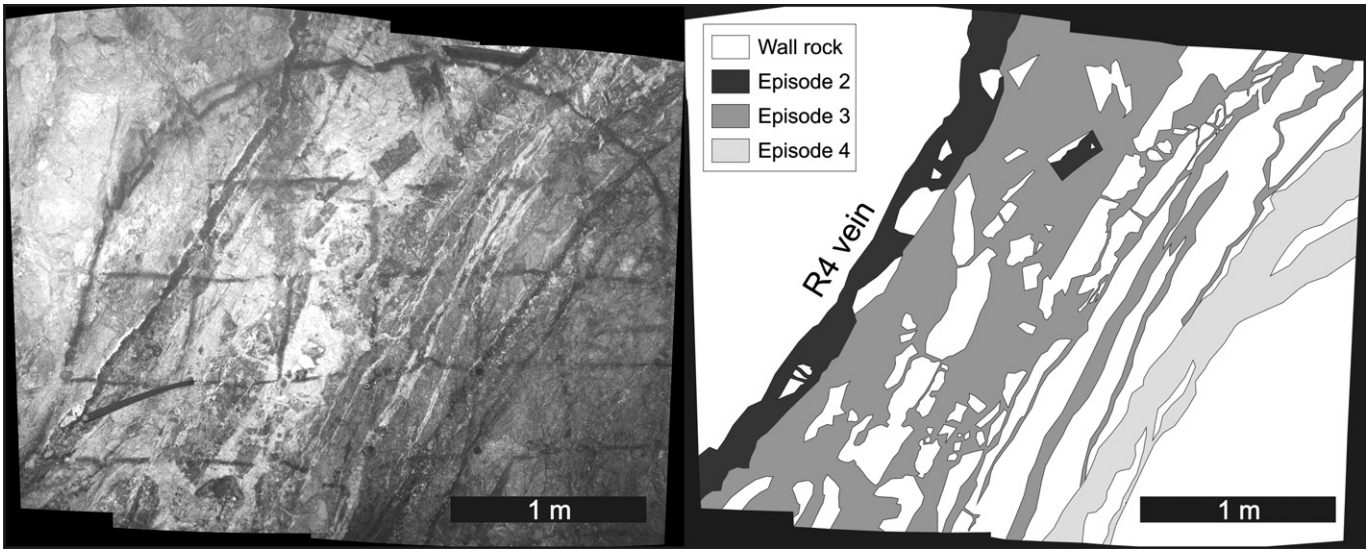

Fig. 4. Photograph and sketch of R4 vein illustrating the relationships between the three main mineralising episodes (underground exposures from 165 m level, view to NW).

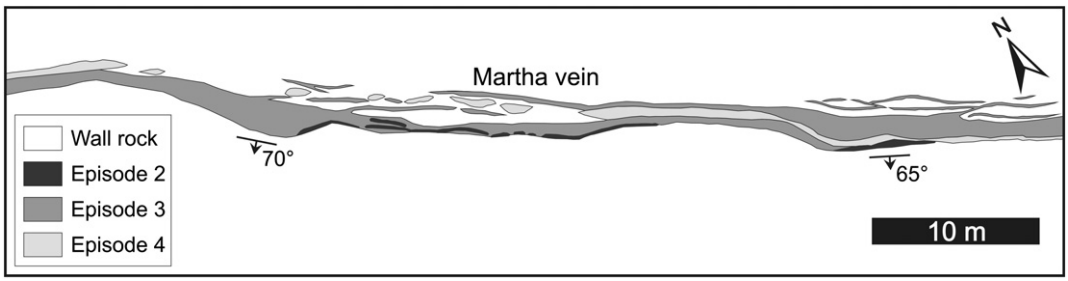

Fig. 5. Map of the paragenetic sequence along the Martha vein, 289 m underground level of Martha Mine (based on maps from Gonzalez Guillot et al., 2004).

4. Martha Mine epithermal deposit

The Martha underground silver deposit is located in the southwestern portion of the Deseado Massif (Fig. 1). The mine is operated by Coeur d'Alene Mines Corporation and has been under production since 2001. Silver concentrations are very high grade, such that in 2002 the mine was ranked 15th amongst the world's silver producers (www.silverinstitute.org). It has produced more than 21 million oz of silver (more than 50% of the Deseado Massif's total silver production) and over 28,000 oz of gold, with an average grade of about 3500 g/t Ag and almost 5 g/t Au (Páez et al., 2008; Sims, 2010).

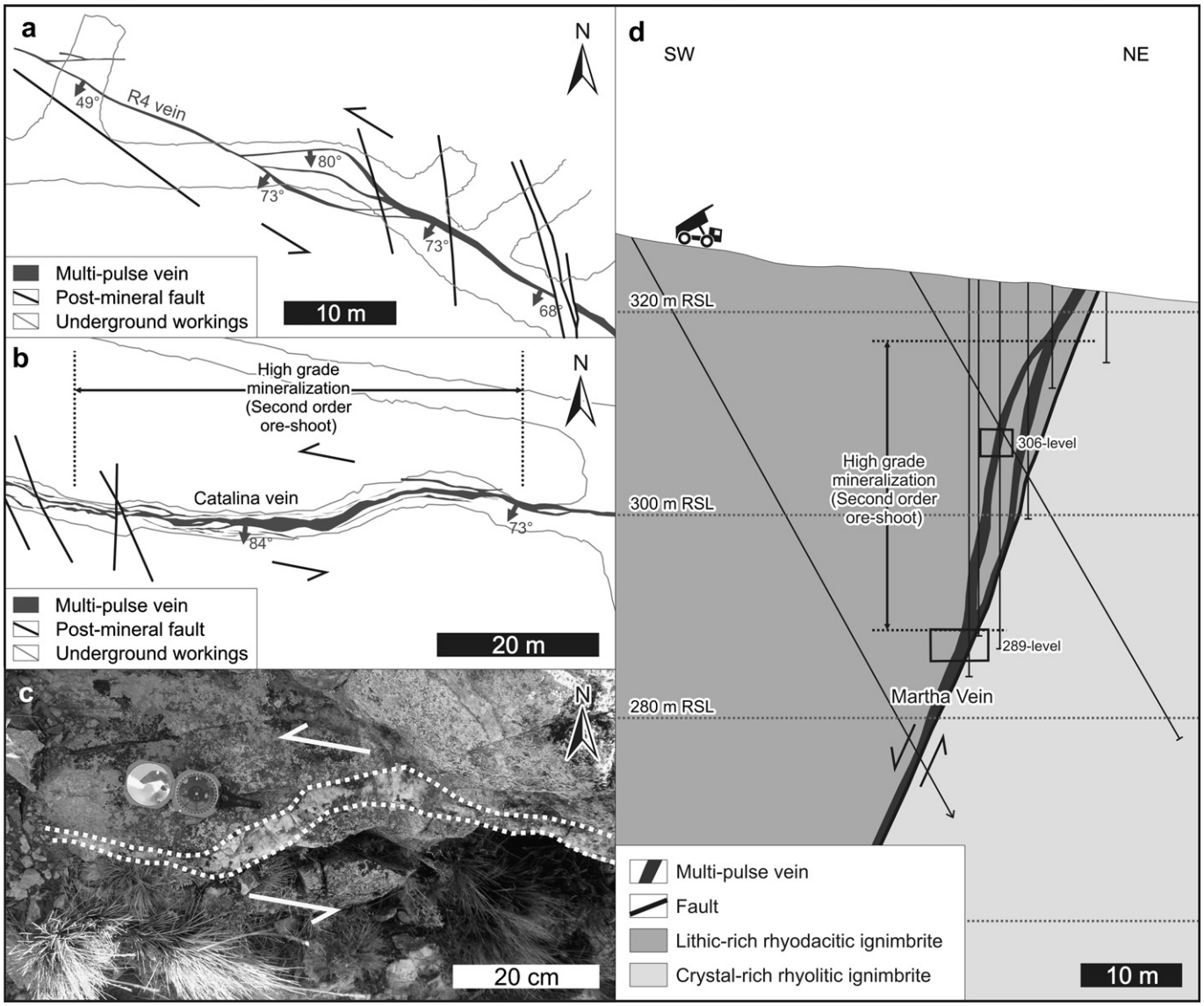

Fig. 6. Sigmoidal jogs and hard-linked step-overs within individual veins. (a) Geological map of a hard-linked step-over within two underlapping segments of R4 vein, 280 m underground level. (b) Geological map of a dilatational jog developed on Catalina vein, 170 m underground level. (c) Surface photograph of a small sized dilatational jog from Catalina Vein. (d) Cross-section of a dilatational jog structure within Martha vein.

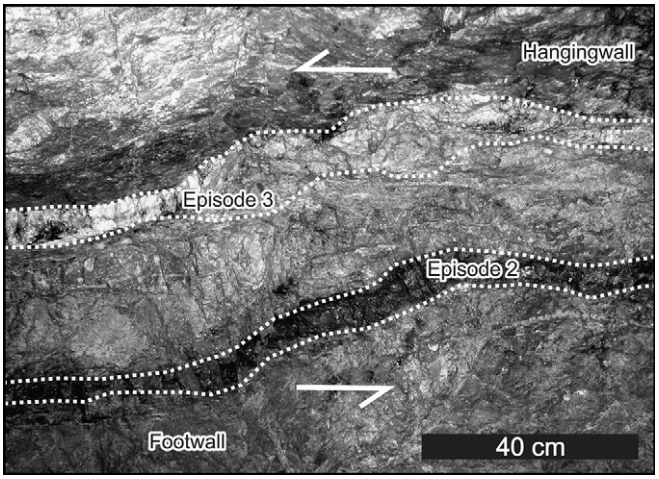

Fig. 7. Photograph of Belén vein showing two dilatational jogs filled with different hydrothermal episodes (underground exposures from 170 m level).

Mineralisation is hosted in Jurassic acid volcanic rocks of the BLVC that are locally represented by thick ash flow tuffs (Fig. 2) with thin intercalations of epiclastic sediments derived from a pyroclastic source (tuffites). In total, mineralisation extends across a 300 m-thick volcanic section (Fig. 2b), which is located on the southern edge of a 10 km diameter Jurassic caldera collapse structure (Ruiz et al., 2008; Páez et al., 2010).

The oldest geological unit is a crystal-rich dacitic ignimbrite (Fig. 2b), which is overlain by a thin tuffaceous unit (Páez et al., 2010). Upwards in the sequence there is a crystal-rich rhyolitic ignimbrite followed again by a thin layer of tuffaceous sediments. The upper part of the sequence is composed of a lithic-rich rhyodacitic ignimbrite related to the caldera-forming volcanic event. The entire sequence dips about 10° towards the NE (Páez et al., 2010). Most of the high-grade ore bodies are developed in the crystal-rich and tuffaceous units (Sims, 2010).

4.1. Vein distribution, extent and continuity

The Martha deposit is composed of more than 15 different veins, 8 of which show high-grade ore-shoots: Martha, R4, Isabel, Nordeste, R4-A, Catalina, Francisca and Belén (Fig. 2a). High-grade mineralisation (up to 40,000 g/t Ag) has been documented, surrounded by a restricted alteration halo of adularia + illite ± smectite (Cedillo Frey et al., 2009; Bauluz et al., 2010). $^{39}Ar/^{40}Ar$ dating on vein adularia reported a 154 Ma age, confirming that the Martha deposit was formed during the Late Jurassic (Sims, 2010).

Martha Mine veins can be grouped into three major vein trends according to their general orientation and location. First, the main NW–SE trending veins, including Martha Oeste, Martha, R4, Martha Este, Martha Sur and Sugar Hill form a structure referred to as the Martha-R4 vein trend (Fig. 2a). Second, in a parallel array but towards the east, the Isabel and Isabel Oeste veins represent the Isabel vein trend (Fig. 2a). Third, the Del Medio vein trend represents all the E–W trending veins (Fig. 2a) including Nordeste, R4A, Belén, Francisca, Catalina and Futuro, and is located within a horst structure defined by the Martha-R4 and Isabel structures (Fig. 2b).

As can be seen in Fig. 2a, Martha and R4 veins are two segments of a single NW–SE trending structure, and together they comprise the high-grade portion of the Martha-R4 vein trend. This portion has a 600 m along-strike extent in discontinuous outcrops. Mineralisation has been reported down to depths of about 250 m below surface (Sims, 2010). This moderately dipping structure has a mean orientation of 206/67 (Fig. 3a), characterised by substantial changes in dip (up to 30°) over short vertical intervals (Fig. 3b). The vein itself is composed of a 1.5–5 m thick, dense network of anastomosing veins and veinlets that are partially developed within a 10 m thick fault zone showing up to 150 m of normal displacement (Fig. 2b).

The Del Medio vein trend constitutes a subparallel array of steeply south dipping E–W trending structures (Fig. 2), ranging between 0.5 and 1 m thick and which locally can reach up to 2.5 m, and is characterised mostly by tabular geometries. This vein trend extends 150–450 m along strike, and mineralisation is reported down to depths of about 200 m below surface (Sims, 2010). All structures within this trend show slightly different mean orientations (Belén: 178/79, Catalina: 185/79, Francisca: 191/80, Nordeste: 167/85). However, when considered as a whole, a mean direction of 184/80 can be determined for the entire trend (Fig. 3c), and it maintains a steep dip with depth (Fig. 2d). This main direction is accompanied by two secondary directions (160/75 and 206/67) that can be identified on maps (Fig. 3e), but are masked in the contour plot (Fig. 3c) by a predominance of measurements on the main direction. These secondary directions are subordinated in most structures, but they may become an important component of

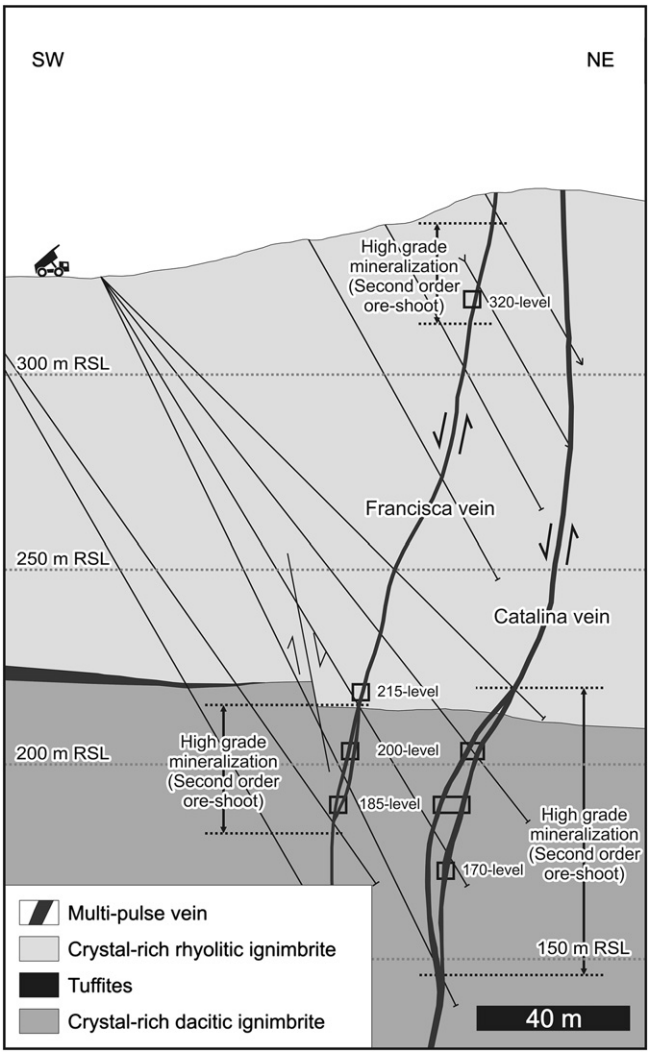

Fig. 8. Cross-section showing relationships amongst lithology, dilatational jogs and high-grade mineralisation in Catalina and Francisca veins.

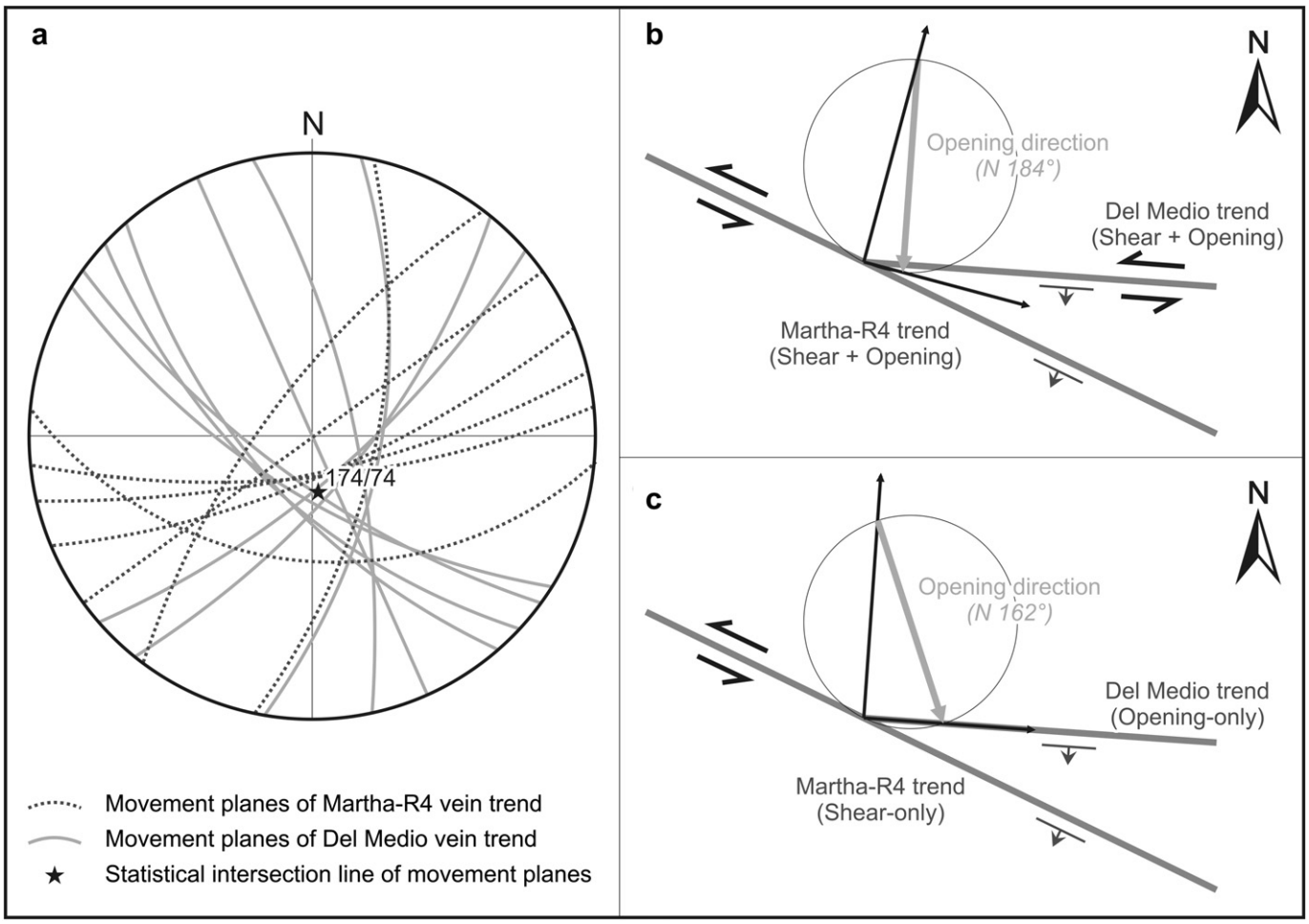

Fig. 9. (a) Determination of the opening vector from the intersection of movement planes of both vein trends, following the Nortje et al. (2006) method. (b) Geometrical construction following McCoss (1986) for both vein trends carrying equal amounts of shear and dilatation. (c) Geometrical construction following McCoss (1986) with the Martha-R4 trend showing only shear and the Del Medio trend pure dilatation.

some structures, as is the case for the 160/75 direction in Nordeste vein (Fig. 2a), or the ~200 m long segment of the Belén-Francisca vein that is parallel to the Martha-R4 vein (Fig. 3e).

The Belén and Francisca veins are part of a unique geometry because they intersect the Catalina vein without offsetting or cross-cutting it, forming a distinct "x" shaped array (Fig. 3e). These structures link with the Martha-R4 vein, changing in orientation as they approach the R4 vein, and merging with it at moderate angles (Fig. 3e). All veins within the Del Medio trend occur in the footwall of the Martha-R4 vein (Figs. 2a, 2b, and 3e). However, in contrast to the Martha-R4 vein, they are not deposited along pre-existing fault zones, as no previous fault rocks have been documented along these structures.

4.2. Vein paragenesis

Martha is an epithermal deposit with a complex mineralogy dominated by Ag–As–Sb sulphosalts and Cu–Pb–Zn sulphides (Gonzalez Guillot et al., 2004, 2008; Márquez-Zavalía et al., 2008). Veins are characterised by a high Ag/Au ratio of about 800:1 (Schalamuk et al., 2002; Sims, 2010).

Mineralised structures at Martha are characterised by a complicated history of fracturing and cementation, arranged in nine paragenetic stages that can be grouped into four episodes (Table 1, Figs. 4 and 5). The similarity and continuity of the hydrothermal infill on the two main vein trends, and the absence of crosscutting relationships between them, suggest that all veins were formed during the evolution of the same hydrothermal system.

The first episode (E_1) is characterised by a barren quartz adularia vein network with no associated sulphides and is poorly represented within the deposit (Table 1). The second episode (E_2) comprises four stages with a progressively decreasing sulphide content (Table 1), ranging from a massive sulphide stage to an almost sulphide-free stage. This episode is responsible for most of the high-grade ore, which is composed of silver and base metal-bearing sulphides and sulphosalts (Table 1). Gangue minerals associated with E_2 are scarce and composed mostly of adularia with minor quartz and sericite. This episode is typically characterised by brecciated textures; however, some crustiform banding may be present locally.

The third episode (E_3) comprises two barren stages characterised by massive adularia and minor quartz (Table 1). This episode typically produced massive to brecciated textures, which are widespread amongst all vein structures, in most cases contributing up to 95% of the veins by volume.

The fourth and last episode (E_4) is characterised by discontinuous, clast-rich chalcedonic breccias and silver-rich sulphosalt veinlets that partially remobilised the previously deposited metals, mostly due to re-brecciation followed by partial dissolution and re-

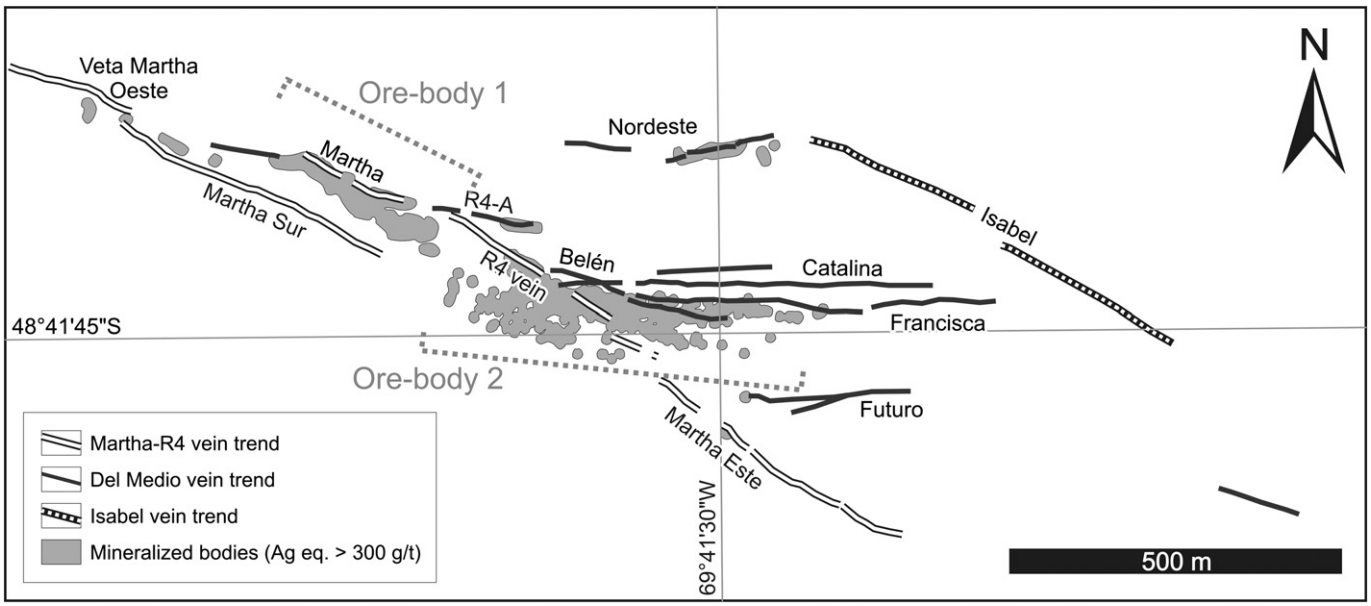

Fig. 10. Map showing the vertical projection of mineralised areas (Ag equivalent >300 g/t) at Martha Mine, Ag equivalent = Ag + 60 × Au. Contouring method: inverse distance to the 3rd power; see Section 3 for details.

precipitation. This episode has highly variable sulphide content (Table 1), showing economic mineralisation only where developed in proximity to E_2. Ore minerals are composed mostly of silver sulphosalts and minor base metal sulfides (Table 1). This final event has a widespread distribution amongst Martha and R4 veins, but is absent amongst the E–W trending structures. Moreover, despite their late nature, breccias associated with this episode can be an important component of the high-grade ore-shoots as they contribute to increase the grade of the mineralisation.

4.3. Distribution of hydrothermal stages within the vein filling

The distribution of the ore-forming episodes was analysed on a 60 m long segment of the Martha vein, at 30 m below surface (289 m level, Fig. 5). This segment of the Martha vein typifies the distribution of hydrothermal episodes in most of the high-grade veins, except for the E_4 episode that is absent in the Del Medio vein trend.

As can be seen in Figs. 4 and 5, the high-grade episode E_2 is mostly developed towards the hanging wall of the vein, and is composed of two separate 20 m and 5 m long segments up to 0.4 m thick. Barren episode E_3 is located close to the footwall of the vein and is characterised by high continuity and thicknesses of up to 2 m. Finally, E_4 is high grade only where it is adjacent to rocks representing the E_2 episode. This final ore-remobilising episode constitutes discontinuous, up to 0.7 m thick, lens-like bodies developed both towards the hanging wall and footwall of the vein, and separated from one another by 1–10 m.

5. Vein geometry and grade distribution

5.1. Vein kinematics

Martha Mine veins are characterised by small bends, sigmoidal jogs and hard-linked step-overs (Fig. 6). These structures commonly range in size from several metres long to a sub-metre-scale, and are developed both along strike and down-dip in all mineralised structures (Figs. 6–8). Where E_2 and E_3 cementation episodes form within separate structures, they show similar normal-sinistral dilatational jog geometry (Fig. 7), indicating that both cementation episodes developed under a similar kinematic regime.

Textural differences can be recognised in the vein rock cementing jogs developed in different vein trends. Dilatational jogs developed in the Martha-R4 vein trend are typically several metres long and mostly dominated by brecciated textures, with crustiform banding and open spaces strongly restricted or absent. By contrast, dilatational jogs in the Del Medio vein trend are commonly smaller but dominated by large (up to 70 cm) drusy cavities and open spaces in the central portions of jogs, along with well-developed crustiform banding. Textural differences possibly reflect higher ratios of dilatation relative to shear in the Del Medio trend compared with the Martha-R4 trend.

Due to lack of slickensides and slickenfibers in most veins, kinematic analysis of vein structures was based on vein geometry and the application of geometric methods developed by Nortje et al. (2006) and McCoss (1986). Nortje et al. (2006) created a stereonet based methodology for reconstructing the vein-opening vector using the three-dimensional geometry of vein deflections (Nortje et al., 2006). Vein deflections are junctions between two single, planar and differently oriented vein segments. For vein segments of different orientation and thickness to be linked, it is likely that they may have been opened in the same phase of deformation (Nortje et al., 2006). At Martha, this assumption is supported by continuity of hydrothermal fillings on both sides of the deflections. Also we make the assumption that vein walls are parallel over the analysed length of each vein segments.

A total number of 16 vein deflections were analysed, 7 for the Martha-R4 vein trend and 9 for the Del Medio vein trend. Both vein trends were analysed together in order to maintain the statistical significance of the results. This analysis relied on the inference that both vein trends developed during evolution of the same hydrothermal system under the same tectonic regime, as discussed above. The stereonet based reconstruction of the opening vectors defines a mean line plunging 174/74 for all considered veins (Fig. 9a). This resulting opening vector plunges steeply to the south and is at a low angle to the vein walls, indicating a large shear component during vein formation (Nortje et al., 2006).

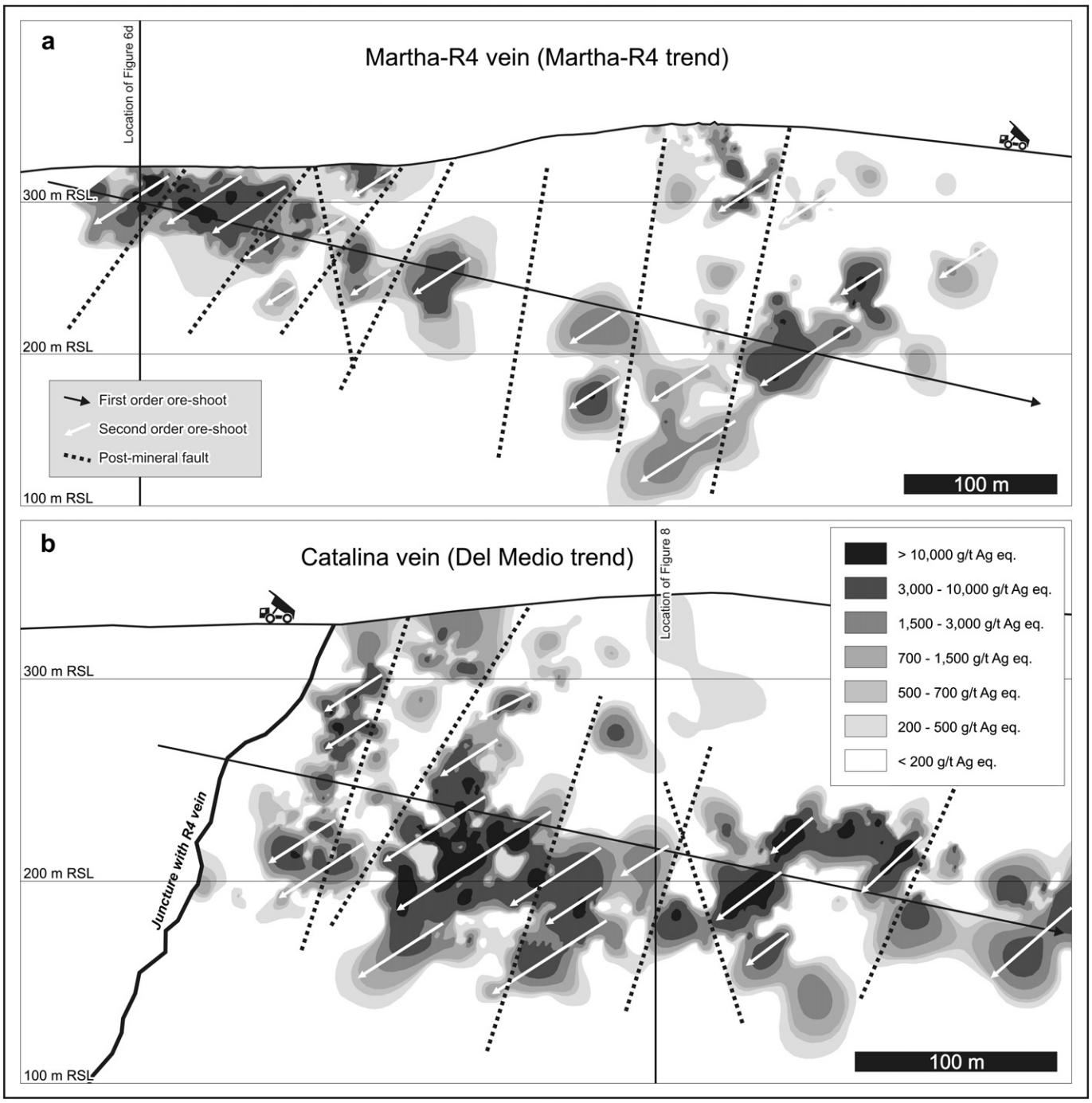

Fig. 11. Longitudinal sections from Martha-R4 (Martha-R4 trend) and Catalina (Del Medio trend) veins showing Ag equivalent grades; Ag equivalent = Ag + 60 × Au. Contouring method: Inverse distance to the 3rd power; see Section 3 for details.

In addition, the graphic approach of McCoss (1986) was applied in order to evaluate the opening vector of the structures and to compare it with results of Nortje et al. (2006) method. This technique is based on determination of two main directions within the vein system, i.e. the greatest shear and dilatation directions, using the mean orientation of each vein trend. Unfortunately this method only gives a 2D direction, which should be approximately equivalent to the horizontal component of the 3D vector determined using the Nortje et al. (2006) method.

In order to establish the greatest shear and dilatation directions for application of McCoss's (1986) method, two contrasting scenarios were taken into consideration. Vein textures in both trends exhibit features suggesting both shearing and extension. However, the Del Medio vein trend seems to show greater ratios of dilatation relative to shear when compared to the Martha-R4 vein trend (e.g. crustiform banding and drusy cavities in Del Medio vein trend infill). Consequently, the kinematic behavior lies between two end-member possibilities. The first is based on the assumption that both vein trends host equal amounts of shear and dilatation (Fig. 9b); whereas the second possibility considers that the Martha-R4 contains the entire shear component and the Del Medio the entire dilatation component (Fig. 9c). The result of applying the

McCoss (1986) graphic construction to these two possibilities indicates that the opening vector for both vein trends has an azimuth between N184° and N162°, with a mean value of N173° (Fig. 9b and c).

Both geometric methods indicate that all considered veins accommodated strain during a transtensional event. The opening vector was directed towards the SSE (Fig. 9), with a mean orientation of 174/74 according to the Nortje et al. (2006) method, and N173° by the McCoss (1986) method. When decomposing the calculated vector on the Martha-R4 and Del Medio vein trends, the result is a strong normal-sinistral kinematic component for the former, compared with a subordinated sinistral component for the latter. Moreover, the opening component should be higher in the Del Medio vein trend as the opening vector is developed more perpendicular to the vein strike. These geometrical conclusions are consistent with the jog and step-over geometry (Figs. 6–8), as well as with the textural differences in jog filling recognised in both vein trends.

5.2. Ore-grade distribution

Ore-shoots at Martha Mine are irregular and discontinuous bodies characterised by silver-rich mineralisation accompanied by gold, base metals, arsenic and antimony (Gonzalez Guillot et al., 2004; Sims, 2010). They typically show average grades around 3500 g/t Ag; the highest grades can reach up to more than 40,000 g/t Ag (Schalamuk et al., 2002; Páez et al., 2008; Sims, 2010). Different scales of ore-shoots can be recognised in both vein trends.

At a deposit scale (several hundreds of metres), two main "multi-vein" mineralised bodies can be identified (Ore-body 1 and Ore-body 2; Fig. 10), along with several other minor bodies. Most ore bodies are developed close to vein intersections and they progressively close away from those intersections.

At the single-vein scale (tens to hundreds of metres), two types of ore-shoots can be identified on longitudinal sections of the Martha-R4 and Del Medio vein trends (Fig. 11), based on their size and orientation. First-order ore-shoots are developed as broad areas extending almost the entire length of veins. They typically have surfaces exceeding 15,000 m^2 and are dominated by medium to high silver grades. However, they are quite irregular in shape and include some low-grade portions. These ore-shoots are characterised by a very gentle plunge of less than 10° towards the SE. Second-order ore-shoots are smaller, with surface areas normally not exceeding 2500 m^2, and they are defined by the high-grade portions of the first-order ore-shoots. These shoots form very high-grade silver bodies, which plunge 30–40° towards the SW.

Figs. 6b, 6d and 8 show how many high-grade areas are associated with dilatational jogs and step-overs, affiliated mostly with subvertical vein segments. The close relationship between jogs and second-order ore-shoots can be recognised when comparing the location of high-grade portions of Catalina (Fig. 8) and Martha vein (Fig. 6d) on the longitudinal sections of silver grades (Fig. 11).

6. Post-mineral modifications

Surface recognition of faults is very difficult in the Deseado Massif as most fault zones have poor outcrops. Most of them can be induced from lineaments on satellite imagery or by the displacement of pyroclastic rocks, and only in some cases from the observation of silicified fault breccias. The presence of underground workings is a unique opportunity to observe and measure fault planes and zones. Post-mineral faulting at Martha Mine crosscut veins and their alteration haloes, with or without any apparent offset of veins (Fig. 12a and b). Two different fault zone styles have been recognised: clast-supported fault breccias and clay-rich gouges.

Clast-supported fault breccias are characterised by clast-supported polymictic breccias with sub-angular fragments. Host rock and vein clasts range in size from sub-millimetric to 6 cm wide, and in some cases small cavities can be found amongst them. These breccias are typically coated with reddish oxides derived from supergenic ore and host rock oxidation. This kind of fault-related breccia shows thicknesses typically varying from 0.3 to 1 m with irregular contacts, and likely represents late reactivation of vein planes because they only have been found in concordance with these structures.

The second fault type is composed of gouge-rich fault zones with sharp contacts. These clay-rich fault zones occasionally are accompanied by fine-grained disseminated pyrite. This kind of structure yields thicknesses ranging between 0.5 cm and 1 m, and can be developed both in a parallel or oblique array with respect to pre-existing veins. These structures originated both as reactivations of pre-existing vein surfaces or as newly formed faults.

At Martha Mine, most post-mineral faults can be related to reactivation of vein planes, as can be seen when comparing the orientations of these structures (Fig. 12c) with those of the mineralised veins (Fig. 12d). Despite that, two new faulting directions can also be identified in Fig. 12a and b. The first reveals a NNW–SSE to N–S orientation and mostly dipping with high angle to the E, and in some cases also to the W. The second direction shows a NW–SE trend, mostly with high angle dips towards the W. Mutually crosscutting relationships and a lack of kinematic indicators suggest that both fault sets were coeval.

6.1. Effects of post-mineral faults

The most important effect that post-mineral faults had over the mineralisation was to displace the ore bodies, juxtaposing high and low grade portions of the same vein, thereby increasing the irregularity of ore-shoots. In this scheme and based on textural attributes, the late remobilising E_4 episode probably represents overlap between late mineralising stages and the first tectonic reactivations of the vein hosting structures.

Another important effect was the generation of preferential pathways for descending meteoric waters, locally increasing the depth of the oxidised horizon of the deposit from about 20 m to more than 100 m. The combined effect of faulting and oxidation resulted in significant ore destruction, and is reflected in a notable grade decrease at the proximities of most post-mineral faults. This effect can be observed as low-grade areas in the vertical projections of silver grades (Fig. 11).

7. Concluding remarks

Fluid migration in shallow crustal environments is strongly influenced by the structural components of the rock mass and their connectivity, defined by structural discontinuities, especially the interconnection of faults, joints, bedding surfaces, foliations, etc. (Sibson, 1996; Cox, 2005). Detailed mapping of veins along with structural elements, such as jogs and step-overs, and the distribution of paragenetic stages, are powerful tools for studying the evolution of hydrothermal systems (Gemmell et al., 1988; Berger et al., 2003; Kreuzer, 2004; Begbie et al., 2007; Kolb and Hagemann, 2009; Wallier, 2009; Micklethwaite, 2009).

Based on field mapping, vein infill study, vein opening analysis, and ore-shoot distribution, the Martha Mine vein system is interpreted as a sinistral transtensive horst structure delimited by the Martha-R4 and Isabel structures (Figs. 2 and 13a). Within this model, the geometries of the three main vein trends are interpreted

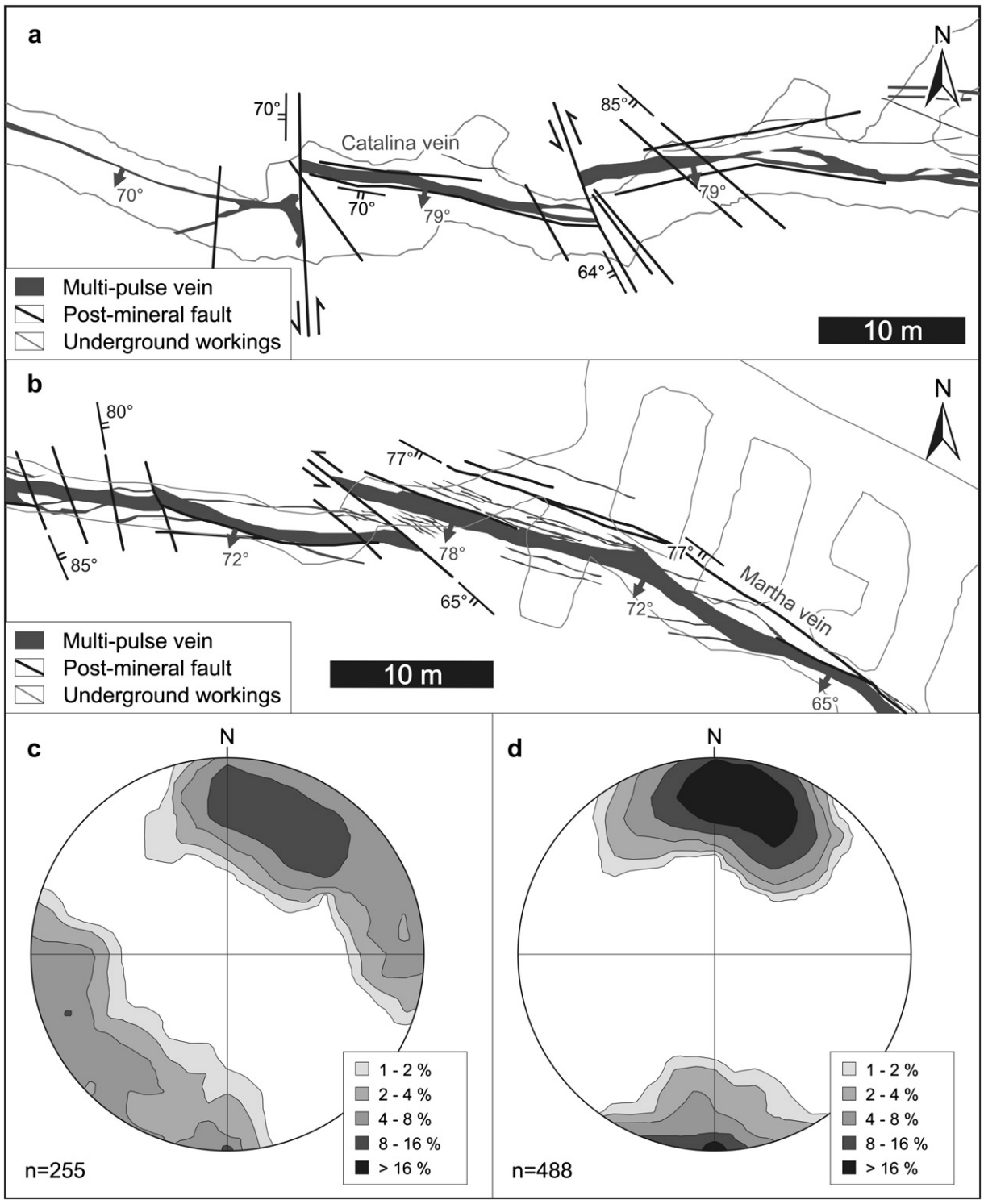

Fig. 12. Post-mineralisation faulting at Martha Mine. (a) Catalina vein, 240 m underground level. (b) Martha vein, 289 m underground level. (c) Post-mineralisation fault orientation (contoured lower hemisphere equal-area stereonet). (d) Orientation of mineralised structures from both vein trends (contoured lower hemisphere equal-area stereonet).

as a hard-linked extensional step-over (Fig. 13a), where the Del Medio vein trend developed as second-order structures in response to growth and linkage of two overlapping, first-order structures composed of the Martha-R4 and Isabel vein trends (see Walsh et al., 1999; Peacock, 2002; Faulkner et al., 2010).

Geometric analyses of Martha Mine veins show a normal-sinistral slip kinematic mode, with an associated opening component for all considered structures. The calculated slip direction (174/74) plunges steeply to the south and is at a low angle to the vein walls, indicating a large shear component during vein formation (Nortje et al., 2006). Vein infill observed in step-overs and jog structures also suggest a normal-sinistral dilatational kinematic for analysed structures (Figs. 6–8), supporting the results of the geometric analysis.

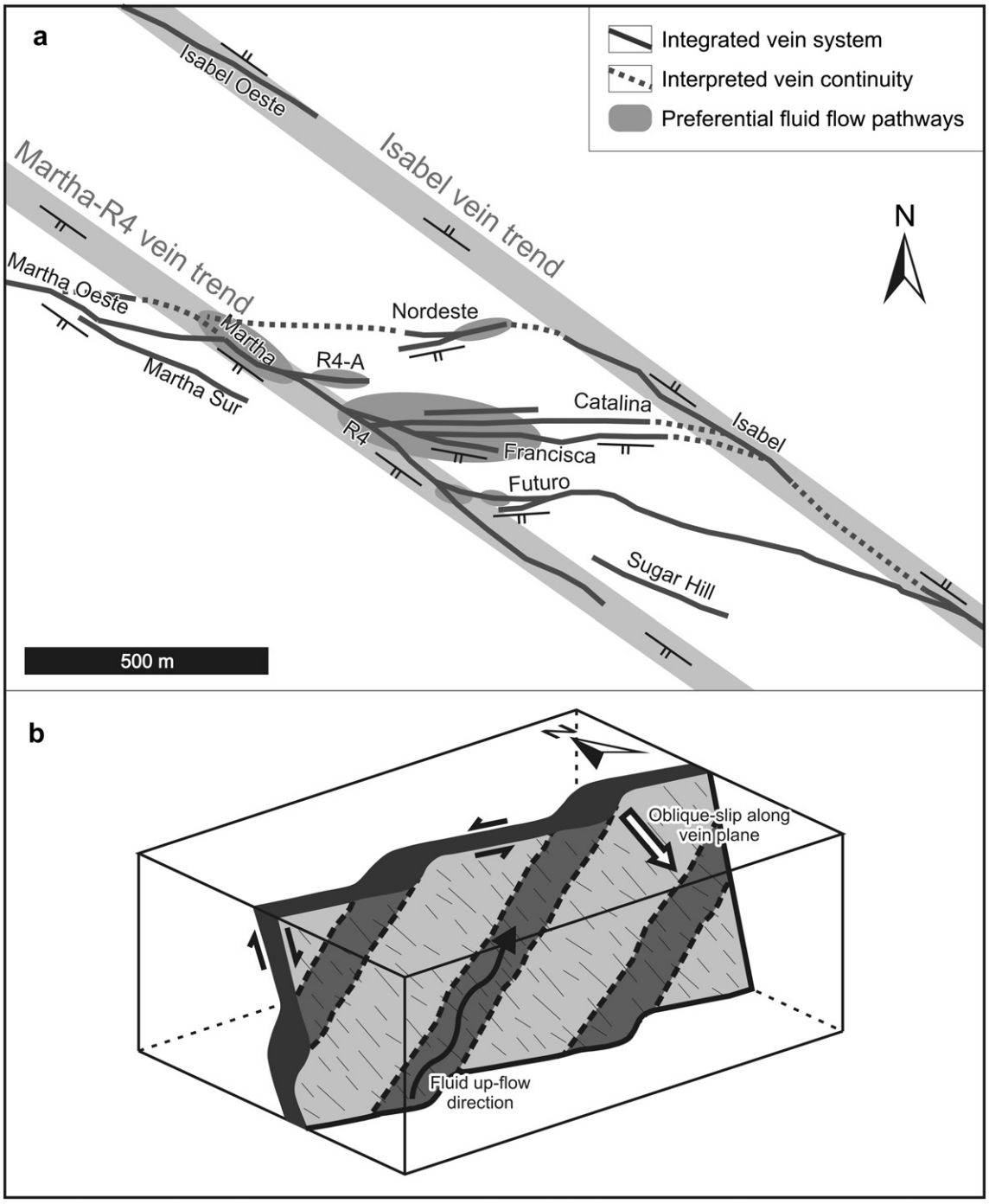

Fig. 13. Structurally controlled fluid flow model for the Martha Mine epithermal deposit. (a) Relationships amongst vein trends and interpreted preferential fluid pathways at the deposit scale. (b) Interpreted hydrothermal flow controlling structures at the single-vein scale.

Continuity of hydrothermal infill within studied veins indicates that all structures were formed during evolution of the same hydrothermal system. However, relationships amongst the different filling episodes indicate progressive vein growth, with multiple episodes of fracturing and cementation (Table 1, Figs. 4 and 5), in a similar manner to other epithermal deposits (e.g. Gemmell et al., 1988; Chauvet et al., 2006; Simmons et al., 2005; Christie et al., 2007; Wallier, 2009).

Based on the geometry and distribution of vein infill, individual veins within Martha-R4 and Del Medio trends may have originated as relatively isolated segments which became part of an integrated structure by propagation and linkage, giving rise to numerous vein-scale jogs and step-overs, both along strike and dip (Figs. 6–8). The final result of this growth mechanism was to produce the curviplanar geometry characteristic of both vein trends (Fig. 3e).

In pyroclastic units, changes in competence may occur from one ignimbrite to another, or within the same unit as a result of variations in the degree of welding (McPhie et al., 1993). In this scheme, jogs and step-overs observed in cross-sections (Figs. 6a and 8) are inferred to represent localized opening areas within individual veins formed in response to vein deflection due to competence contrasts within the vein host rocks (Reid et al., 1975; Ferrill and

Morris, 2003), or the result of down-dip vein linkages through an anisotropic volcanic sequence (Childs et al., 1996).

Ore-shoots at Martha Mine are irregular and discontinuous silver-rich bodies that can reach very high grades (up to more than 40,000 g/t Ag). At the deposit scale, a series of multi-vein ore bodies are observed within the interpreted hard-linked extensional step-over zone, in close affiliation with vein intersections (Fig. 10). Within single veins, mineralisation is represented as broad areas defining gently plunging first-order ore-shoots of irregular shapes, which are a result of the combination of numerous high-grade second-order ore-shoots, which can be individually associated with dilatational jogs and step-overs (Figs. 6b and d, 8, and 11).

The close relationship between high grades and locations of vein intersections, dilatational jogs and step-overs (Figs. 6, 8, 10, and 11) suggest that structure played a significant role during ore deposition, probably controlling preferential pathways for hydrothermal solutions to be focused and concentrated, leading to ore deposition (Sibson, 1996; Berger et al., 2003; Rowland and Sibson, 2004; Cox, 2005).

Based on the proposed structural scheme and grade distribution pattern, a structurally controlled fluid flow model can be delineated for the entire Martha vein system (Fig. 13). At the deposit scale, the up-flowing hydrothermal solutions are interpreted to have been concentrated on the hard-linked step-over zone developed between the two NW master trending structures (Fig. 13a), in a similar way as has been described for many hydrothermal environments (see, e.g., Curewitz and Karson, 1997; Berger et al., 2003; Rowland and Sibson, 2004; Micklethwaite et al., 2010). Within the step-over area, hydrothermal ascending fluids took advantage of intersections within the two main vein trends (Fig. 13a), focusing the hydrothermal outflow, and controlling the generation of first-order ore-shoots (see, e.g., Hulin, 1929; Fernández et al., 2008; Curewitz and Karson, 1997; Cox, 2005). At the scale of a single vein, hydrothermal solutions were ultimately channelized and concentrated along preferred opening areas such as jogs and small sized step-overs (Fig. 13b), resulting in ore deposition and formation of second-order ore-shoots (see, e.g., Newhouse, 1940; Ferrill and Morris, 2003; Kreuzer, 2004; Cox, 2005; Nelson, 2006). Finally the mineralisation was modified by a complex post-mineral faulting event, producing dislocation of ore bodies and segmentation of high-grade ore-shoots.

Hydrothermal flow in epithermal environments is a complex and poorly constrained process; however, most researchers now agree that the presence of highly permeable conduits is an important factor in order to form high grade “bonanza” ore-shoots in shallow crustal levels (Simmons and Browne, 2000; Berger et al., 2003; Cox, 2005; Simmons and Brown, 2006; Micklethwaite, 2009). Hence, Martha Mine epithermal deposit constitutes an excellent example of how structure plays a fundamental role in channelizing and concentrating metal-bearing solutions into small portions of the crust, controlling mineral deposition and the formation of an economic-grade mineral deposit.

Acknowledgements

This work is part of a PhD thesis carried out at the Universidad Nacional de La Plata (UNLP) with the support of Coeur d’Alene Mines and a Hugh E. McKinstry Student Research Award from the Society of Economic Geologists. The authors wish to thank Alfredo Cruzat, Claudio Romo and the Martha Mine staff for their help, discussions and access to data. We also appreciate the support, discussions and constructive suggestions given by Kathy Campbell and Julie Rowland. Finally, the thorough reviews of Steven Micklethwaite and Gustav Nortje, and the editorial assistance of Tom Blenkinsop are gratefully acknowledged.

References

Bauluz, B., Cedillo, A., Subias, I., Páez, G.N., Ruiz, R., Guido, D.M., 2010. Hydrothermal clays at the Futuro Vein, Martha Mine silver epithermal deposit, Deseado Massif, Patagonia, Argentina. Trilateral Meeting on Clays (2010TMC), Abstracts, Spain.

Begbie, M.J., Sporli, K.B., Mauk, J.L., 2007. Structural evolution of the Golden Cross epithermal Au–Ag deposit, New Zealand. Economic Geology 102, 873–892.

Berger, B.R., Tingley, J.V., Drew, L.J., 2003. Structural localization and origin of compartmentalized fluid flow, Comstock Lode, Virginia City, Nevada. Economic Geology 98, 387–408.

Brathwaite, R.L., Cargill, H.J., Christie, A.B., Swain, A., 2001. Lithological and spatial controls on the distribution of quartz veins in andesite- and rhyolite-hosted epithermal Au–Ag deposits of the Hauraki Goldfield, New Zealand. Mineralium Deposita 36, 1–12.

Cedillo Frey, A., Páez, G.N., Ruiz, R., Bauluz Lázaro, B., Subías Pérez, I., 2009. Mineralogía de la alteración hidrotermal en el yacimiento epitermal Mina Martha, Macizo del Deseado, Argentina. Revista de la Sociedad Española de Mineralogía (Macla) 11, 57–58.

Chauvet, A., Bailly, L., André, A., Monié, P., Cassard, D., Tajada, F.L., Vargas, J.R., Tuduri, J., 2006. Internal vein texture and vein evolution of the epithermal Shila-Paula district, southern Peru. Mineralium Deposita 41, 387–410.

Childs, C., Nicol, A., Walsh, J.J., Watterson, J., 1996. Growth of vertically segmented normal faults. Journal of Structural Geology 18, 1389–1397.

Christie, A.B., Simpson, M.P., Brathwaite, R.L., Mauk, J.L., Simmons, S., 2007. Epithermal Au–Ag and related deposits of the Hauraki Goldfield, Coromandel Volcanic Zone, New Zealand. Economic Geology 102, 785–816.

Cox, S.F., 2005. Coupling between deformation, fluid pressures and fluid flow in ore producing hydrothermal systems at depth in the crust. Economic Geology, 1–35. 100th Anniversary volume.

Curewitz, D., Karson, J.A., 1997. Structural setting of hydrothermal outflow: fracture permeability maintained by fault propagation and interaction. Journal of Volcanology and Geothermal Research 79, 149–168.

Echavarría, L.E., Schalamuk, I.B.A., Etcheverry, R.O., 2005. Geologic and tectonic setting of Deseado Massif epithermal deposits, Argentina, based on El Dorado-Monserrat. Journal of South American Earth Sciences 19, 415–432.

Echeveste, H., Fernández, R., Bellieni, G., Tessone, M., Llambias, E., Schalamuk, I., Piccirillo, E., Demin, A., 2001. Relaciones entre las Formaciones Bajo Pobre y Chon Aike (Jurásico medio a superior) en el área de Estancia El Fénix-Cerro Huemul, zona centro-occidental del Macizo del Deseado, provincia de Santa Cruz. Revista de la Asociación Geológica Argentina 56 (4), 548–558.

Faulkner, D.R., Jackson, C.A.L., Lunn, R.J., Schlische, R.W., Shipton, Z.K., Wibberley, C.A.J., Withjack, M.O., 2010. A review of recent developments concerning the structure, mechanics and fluid flow properties of fault zones. Journal of Structural Geology 32 (11), 1557–1575.

Fernández, R.R., Blesa, A., Moreira, P., Echeveste, H., Mykietiuk, K., Andrada de Palomera, P., Tessone, M., 2008. Los depósitos de oro y plata vinculados al magmatismo jurásico de la Patagonia: revisión y perspectivas para la exploración. Revista de la Asociación Geológica Argentina 63 (4), 665–681.

Ferrill, D.A., Morris, A.P., 2003. Dilational normal faults. Journal of Structural Geology 25, 183–196.

Feruglio, E., 1949. Descripción geológica de la Patagonia, 3 vols.. Dirección Nacional de Yacimientos Petrolíferos Fiscales, Buenos Aires.

Gemmell, J.B., Simmons, S.F., Zantop, H., 1988. The Santo Nino silver–lead–zinc vein, Fresnillo District, Zacatecas, Mexico: part I, structure, vein stratigraphy, and mineralogy. Economic Geology 83, 1597–1618.

Giacosa, R., Zubia, M., Sanchez, M., Allard, J., 2010. Meso-Cenozoic tectonics of the southern Patagonian foreland: structural evolution and implications for Au–Ag veins in the eastern Deseado Region (Santa Cruz, Argentina). Journal of South American Earth Sciences 30 (3–4), 134–150.

Gibbs, A.D., 1984. Structural evolution of extensional basin margins. Journal of the Geological Society, London 141, 609–620.

Gonzalez Guillot, M., De Barrio, R., Ganem, F., 2004. Mina Martha, un yacimiento epitermal argentífero en el Macizo del Deseado, provincia de Santa Cruz. In: VII Congreso de Mineralogía y Metalogenia, Actas, pp. 119–204.

Gonzalez Guillot, M., Biel Soria, C., Fanlo Gonzalez, Subías Perez, I., Mateo Gonzalez, E., 2008. Cobres grises y sulfosales de plata del yacimiento epitermal de Mina Martha, Macizo del Deseado, Santa Cruz (Argentina). Revista de la Sociedad Española de Mineralogía (Macla) 8, 127–128.

Guido, D., 2004. Subdivisión litofacial e interpretación del volcanismo jurásico (Grupo Bahía Laura) en el este del Macizo del Deseado, provincia de Santa Cruz. Revista de la Asociación Geológica Argentina 59 (4), 727–742.

Guido, D., Schalamuk, I., 2003. Genesis and exploration potential of epithermal deposits from the Deseado Massif, Argentinean Patagonia. In: Eliopoulos, et al. (Eds.), Mineral Exploration and Sustainable Development, vol. I. Balkema-Rotterdam, pp. 493–496.

Guido, D.M., Jovic, S.M., Schalamuk, I.B., 2005. A new metallogenic association (Sn–Cd–In–Zn–Ag–Au) in the Deseado Auroargentiferous province, Deseado Massif, Patagonia, Argentina. In: Mineral Deposit Research: Meeting the Global Challenge – 8th SGA Meeting, Beijing, China, vol. 2 965–968.

Holcombe, R.J., 2009. Georient v9.4.4, Stereographic Projections and Rose Diagram Software. Department of Earth Sciences, University of Queensland, Australia. Available at: http://www.holcombe.net.au/software/.

Homovc, J., Constantini, L., 2001. Hydrocarbon exploration potential within interplate shear-related depocenters: Deseado and San Julián basins, southern Argentina. American Association of Petroleum Geologist, Bulletin 85 (10), 1795–1816.
Hulin, C.D., 1929. Structural control of ore deposition. Economic Geology 24, 15–49.
Jovic, S.M., Guido, D.M., Schalamuk, I.B., Ríos, F.J., Tassinari, C.C.G., Recio, C., 2010. Pingüino In-bearing polymetallic vein deposit, Deseado Massif, Patagonia, Argentina: characteristics of mineralization and ore-forming fluids. Mineralium Deposita 45, 735–763.
Kolb, J., Hagemann, S., 2009. Structural control of low-sulfidation epithermal gold mineralization in the Rosario–Bunawan district, East Mindanao Ridge, Philippines. Mineralium Deposita 44 (7), 795–815.
Kreuzer, O.P., 2004. How to resolve the controls on mesothermal vein systems in a goldfield characterized by sparse kinematic information and fault reactivation: a structural and graphical approach. Journal of Structural Geology 26 (6-7), 1043–1065.
López, R., 2006. Estudio Geológico-Metalogenético del area oriental al curso medio del Río Pinturas, sector noroeste del Macizo del Deseado, provincia de Santa Cruz, Argentina. Universidad Nacional de La Plata. Unpublished PhD thesis.
Márquez-Zavalía, M.F., Bindi, L., Márquez, M., Menchetti, S., 2008. Se-bearing polybasite-Tac from the Martha Mine, Macizo del Deseado, Santa Cruz, Argentina. Mineralogy and Petrology 94 (1), 145–150.
McCoss, A.M., 1986. Simple constructions for deformation in transpression/transtension zones. Journal of Structural Geology 8 (6), 715–718.
McPhie, J., Doyle, M., Allen, R., 1993. Volcanic textures, a Guide to the Interpretation of Textures in Volcanic Rocks. CODES, University of Tasmania. 196 p.
Micklethwaite, S., 2009. Mechanisms of faulting and permeability enhancement during epithermal mineralisation: Cracow goldfield, Australia. Journal of Structural Geology 31, 288–300.
Micklethwaite, S., Sheldon, H.A., Baker, T., 2010. Active fault and shear processes and their implications for mineral deposit formation and discovery. Journal of Structural Geology 32, 151–165.
Moreira, P., Fernández, R., Cabana, C., Schalamuk, I.A., 2008. Análisis estructural de las mineralizaciones jurásicas del proyecto epitermal La Josefina (Au–Ag), Macizo del Deseado, Santa Cruz. Revista de la Asociación Geológica Argentina 63 (2), 244–253.
Nelson, E.P., 2006. Drill-hole design for dilational ore shoot targets in fault-fill veins. Economic Geology 101, 1079–1085.
Newhouse, W.H., 1940. Openings due to movement along a curved or irregular fault plane. Economic Geology 35 (3), 445–464.
Nicol, A., Walsh, J.J., Villamor, P., Seebeck, H., Berryman, K.R., 2010. Normal fault interactions, paleoearthquakes and growth in an active rift. Journal of Structural Geology 32, 1101–1113.
Nortje, G., Rowland, J., Spörli, K., Blenkinsop, T., Rabone, S., 2006. Vein deflections and thickness variations of epithermal quartz veins as indicators of fracture coalescence. Journal of Structural Geology 28, 1396–1405.
Oliver, N.H.S., Ord, A., Valenta, R.K., Upton, P., 2001. Deformation, fluid flow, and ore genesis in heterogeneous rocks, with examples and numerical models from the Mount Isa District, Australia. Reviews in Economic Geology 14, 51–74.
Páez, G.N., Ruiz, R., Guido, D.M., Schalamuk., I.B., 2008. Historia del yacimiento argentífero Mina Martha, Macizo del Deseado, Santa Cruz. In: XVII Congreso Geológico Argentino, Actas (II), Argentina, pp. 661–662.
Páez, G.N., Ruiz, R., Guido, D.M., Jovic, S.M., Schalamuk, I.B., 2010. Estratigrafía volcánica del yacimiento argentífero Mina Martha, Macizo del Deseado, provincia de Santa Cruz. Revista de la Asociación Geológica Argentina 67 (1), 77–90.
Pankhurst, R., Leat, P., Sruoga, P., Rapela, C., Marquez, M., Storey, B., Riley, T., 1998. The Chon Aike province of Patagonia and related rocks in West Antarctica: a silicic large igneous province. Journal of Volcanology and Geothermal Research 81, 113–136.
Pankhurst, R., Riley, T., Fanning, C., Kelley, S., 2000. Episodic silicic volcanism in Patagonia and the Antarctic Peninsula: chronology of magmatism associated with the break-up of Gondwana. Journal of Petrology 41 (5), 605–625.
Peacock, D.C., 2002. Propagation, interaction and linkage in normal fault systems. Earth-Science Reviews 58, 121–142.
Pollard, D.D., Segall, P., Delaney, P.T., 1982. Formation and interpretation of dilatants echelon cracks. Geological Society of America Bulletin 93, 1291–1303.
Reid, R.R., Caddey, S.W., Rankin, J.W., 1975. Primary refraction control of ore shoots, with examples from the Coeur d'Alene District, Idaho. Economic Geology 70, 1050–1061.
Richardson, N.J., Underhill, J.R., 2002. Controls on the structural architecture and sedimentary character of syn-rift sequences, North Falkland Basin, South Atlantic. Marine and Petroleum Geology 19 (4), 417–443.
Rosendahl, B.R., Reynolds, D., Lorber, P., Burgess, C., McGill, J., Scott, D., Lambiase, J., Derksen, S., 1986. Structural expressions of rifting: lessons from Lake Tanganyika. In: Frostick, L.E., et al. (Eds.), Sedimentation in the East African Rifts. Geological Society of London, Special Publication, vol. 25, pp. 29–43.
Rowland, J.V., Sibson, R.H., 2004. Structural Controls on hydrothermal flow in a segmented rift system, Taupo Volcanic Zone, New Zealand. Geofluids 4, 259–283.
Ruiz, R., Páez, G.N., Guido, D.M., Schalamuk., I.B., 2008. Ambiente volcánico y mineralizaciones del Área Cerro 1ro de Abril, Sector Sudoccidental del Macizo del Deseado, Santa Cruz, Argentina. In: XVII Congreso Geológico Argentino, Actas (II), Jujuy, Argentina, pp. 897–898.
Sibson, R.H., 1996. Structural permeability of fluid-driven fault-fracture meshes. Journal of Structural Geology 18 (8), 1031–1042.
Sillitoe, R.H., Hedenquist, J.W., 2003. Linkages between volcanotectonic settings, ore fluid compositions, and epithermal precious metal deposits. In: Society of Economic Geologists, Special Publication, vol. 10, pp. 315–343.
Simmons, S.F., Browne, P.R.L., 2000. Hydrothermal minerals and precious metals in the Broadlands-Ohaaki geothermal system: implications for understanding low-sulfidation epithermal environments. Economic Geology 95, 971–999.
Simmons, S.F., White, N.C., John, D.A., 2005. Geological characteristics of epithermal precious and base metal deposits. Economic Geology, 485–522. 100th Anniversary volume.
Simmons, S.F., Brown, K.L., 2006. Gold in magmatic hydrothermal solutions and the rapid formation of a giant ore deposit. Science 314, 288–291.
Sims, J., 2010. Martha Mine, Santa Cruz, Argentina. NI 43-101 Technical Report. 105 p. Available at: http://www.sedar.com.
Schalamuk, I., Zubia, M., Genini, A., Fernández, R., 1997. Jurassic epithermal Au–Ag deposits of Patagonia, Argentina. Ore Geology Reviews 12 (3), 173–186.
Schalamuk, I., de Barrio, R., Zubia, M., Genini, A., Echeveste, H., 1999. Provincia Auroargentífera del Deseado, Santa Cruz. In: Zappettini, E. (Ed.), Recursos Minerales de la República Argentina. Instituto de Geología y Recursos Minerales SEGEMAR, Anales 35, 1177–1188.
Schalamuk, I., de Barrio, R., Zubia, M., Genini, A., Valvano, J., 2002. Mineralizaciones auroargentíferas del Macizo del Deseado y su encuadre metalogénico, provincia de Santa Cruz. In: Haller, M. (Ed.), Geología y recursos minerales de Santa Cruz. Relatorio XV Congreso Geológico Argentino, Buenos Aires, IV-2, pp. 679–714.
Wallier, S., 2009. The geology and evolution of the Manantial Espejo epithermal silver (+gold) deposit, Deseado Massif, Argentina. Unpublished PhD thesis, University of British Columbia, Vancouver, Canada. 303 p.. Available at: http://circle.ubc.ca/handle/2429/17439.
Walsh, J.J., Watterson, J., Bailey, W., Childs, C., 1999. Fault relays, bends and branch-lines. Journal of Structural Geology 21, 1019–1026.
Walsh, J.J., Bailey, W.R., Childs, C., Nicol, A., Bonson, C.G., 2003. Formation of segmented normal faults. Journal of Structural Geology 25, 1251–1262.